Response of stepped conical shells to the blast loading

Jaan Lellep and Ella Puman

***Abstract*—** Problems of the blast loading of inelastic plates and shells have theoretical and practical importance. The plastic response of a conical shell to the blast loading is studied. Material of the shell is assumed to be a perfect plastic material. Piece wise linear approximations of the exact yield surface are used. Making use of the velocity field corresponding to the associated flow law the statically admissible field of stress resultants is constructed. For determination of residual deflections the method of mode form motions is applied. Numerical results are obtained for the exponentially decaying load intensity.

***Keywords*—**blast loading, conical shell, plasticity, stepped thickness.

I. Introduction

The blast and impact loading of structural elements occurs in various situations of the real life including vehicle accidents, metal forming and so on. Evidently, in the cases of a blast loaded structure the role of elastic deformations is often negligible.

That is why in modelling of the material behavior of structures and structural elements subjected to the blast or impact loading the use of the concept of a rigid-plastic body is justified (see Jones [5]). An excellent example of the solution procedure was developed by Hopkins and Prager [4] who obtained the exact solution for a rigid plastic circular plate subjected to the rectangular impulse. Later this concept was extended to other types of structural elements by many authors. Stronge and Yu [20] concentrated at the dynamic plastic behavior of beams and arches.

The plastic response of plates and shells to impact and blast loading is investigated by Jones [5], Shen, Jones [18], Chakrabarty [1], Duffey [2], Kaliszky [6], Martin [15] and others.

The solutions of the problems of limit analysis of circular conical shells are obtained by Hodge [3], Kuech and Lee [7], Lance and Lee [8], Onat [16]. Lellep and Puman [9-12] developed minimum weight designs for shells with piece wise constant thickness loaded by a rigid central boss and by the distributed lateral loading. Ross [17] has studied, both, elastic and inelastic shells and has concentrated at the problems of stability of conical shells with stiffeners.

The research was partly supported by the Grant Nº 9110 of the Estonian Science Foundation and by the institutional research funding IUT 20-57 of the Estonian Ministry of Education and Research.

J. Lellep is with the Institute of Mathematics, University of Tartu, 50409, Tartu, Estonia (phone: +372-737-5868; e-mail: jaan.lellep@ut.ee).

E. Puman is with the Institute of Mathematics, University of Tartu (e-mail: ella.puman@ut.ee).

Much less attention has been paid in the literature to conical shells subjected to dynamical loading. Lellep and Puman [13, 14] studied the inelastic response of conical shells to the rectangular impulse and to the blast loading.

In the present paper a theoretical method for determination of residual deflections of blast loaded inelastic conical shells with stepped thickness is developed. The formulation of the problem with basic hypotheses and integration of basic equations with numerical results are presented in detail.

II. Problem Formulation

The dynamic plastic response of circular conical shells will be studied under the assumption that the stress strain state remains axisymmetric during the deformation. The loading is assumed to be a blast loading. Let the shell be simply supported at the outer edge for radius $r = R$ and let the inner edge at $r = a$ be completely free (Fig.1-2). Here r stands for the current radius. The thickness of the shell wall is assumed to be equal to the constant h_j in the segment (a_j, a_{j+1}) for each $j = 0, \dots, n$. It is reasonable to denote $a = a_0$ and $R = a_{n+1}$. Thus

$$h = h_j \tag{1}$$

for $r \in (a_j, a_{j+1}); j = 0, \dots, n$. The parameters a_j, h_j are considered as given constants.

Let the intensity of the uniformly distributed transverse loading be $P(t)$ while

$$P(t) = \begin{cases} p_0 g(t), & t \in [0, t_0] \\ 0, & t > t_0 \end{cases} \tag{2}$$

where p_0 is a given constant and $g(t)$ – a decreasing function of time t.

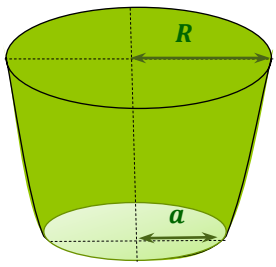

Fig. 1. Middle surface of the shell

It is assumed as shown in (2) that an abrupt unloading takes place at the time instant t_0. The subsequent motion of the material is due to the inertia.

The aim of the paper is to prescribe the stress strain state of the shell during the motion. Note that elastic deformations and strain hardening are assumed to be negligible. The geometrically linear theory of thin shells made of perfectly plastic materials will be employed. This theory admits to build up a piece wise linear field of kinematically admissible transverse velocities and to determine corresponding membrane forces and bending moments.

III. Generalized Stresses and Strains

In the classical bending theory of plates and shells the stress components contributing the strain energy are bending moments M_1, M_2 and membrane forces N_1, N_2 in the transversal and circumferential directions, respectively.

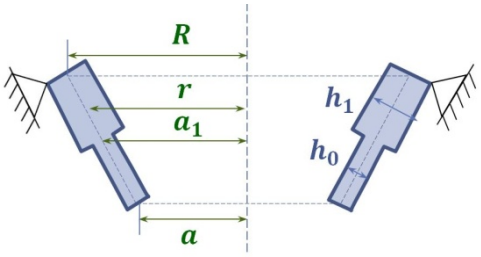

Fig. 2. Conical shell with piece wise constant thickness

Let the dots denote the differentiation with respect to time and prims with respect to the current radius. The displacements U and V in the radial and circumferential directions are assumed to be small in comparison to the transverse deflection W and corresponding inertial terms will be neglected.

The strain energy rate per unit area of the middle surface can be presented as (see Hodge [3], Jones [5])

$$\dot{D}_0 = N_1\dot{\varepsilon}_1 + N_2\dot{\varepsilon}_2 + M_1\dot{\varkappa}_1 + M_2\dot{\varkappa}_2. \tag{3}$$

Here $\dot{\varepsilon}_1$ and $\dot{\varepsilon}_2$ stand for the linear strain rates in directions "one" and "two" whereas $\dot{\varkappa}_1$ and $\dot{\varkappa}_2$ are the corresponding curvature rates. The total internal energy dissipation equals

$$\dot{D}_i = \int_0^{2\pi}\int_a^R \dot{D}_0\, r dr d\theta. \tag{4}$$

The power of external loads is

$$\dot{D}_e = \int_0^{2\pi}\int_a^R \left(P - \mu h\ddot{W}\right) r dr d\theta. \tag{5}$$

provided the inertial forces in the longitudinal and circumferential directions can be neglected.

The principle of virtual work may be expressed as

$$\dot{D}_i = \dot{D}_e. \tag{6}$$

In what follows we shall study the symmetrical behavior of a conical shell within the limits of the linear bending theory of thin shells. That is why the shear forces Q_1, Q_2 as well as stress resultants N_{12}, M_{12} are absent in (3).

The strain rates included in (3) must be in consistent with corresponding generalized stresses. It can be shown that (see Hodge [3], Kaliszky [6])

$$\begin{aligned}
\dot{\varepsilon}_1 &= \frac{d\dot{U}}{dr}\cos\varphi\,,\\
\dot{\varepsilon}_2 &= \frac{1}{r}\left(\dot{U}\cos\varphi + \dot{W}\sin\varphi\right),\\
\dot{\varkappa}_1 &= -\frac{d^2\dot{W}}{dr^2}\cos^2\varphi\,,\\
\dot{\varkappa}_2 &= -\frac{1}{r}\frac{d\dot{W}}{dr}\cos^2\varphi\,.
\end{aligned} \tag{7}$$

Here φ stands for the angle of inclination of a generator of the middle surface of the shell (Fig. 2).

The use of the principle of virtual work (6) with (3)–(5) furnishes the equilibrium conditions

$$\begin{aligned}
&\frac{d}{dr}(rN_1) - N_2 = 0,\\
&\frac{d}{dr}(rQ) - N_2\tan\varphi + \frac{r\left(P - h\,\mu\ddot{W}\right)}{\cos\varphi} = 0,\\
&\frac{d}{dr}(rM_1) - M_2 - \frac{rQ}{\cos\varphi} = 0,
\end{aligned} \tag{8}$$

where Q is the radial shear force.

Note that the equilibrium equations (8) can be derived directly using the equilibrium conditions of a shell element loaded by the internal and external forces (the latters are the inertial force and the lateral transverse pressure). However, the internal generalized forces include the moments M_1 and M_2 and membrane forces N_1, N_2.

It is easy to eliminate the shear force Q from the system (8) and present the last equations in (8) as

$$\begin{aligned}
\frac{d}{dr}\left[\frac{d}{dr}(rM_1) - M_2\right] - N_2\frac{\sin\varphi}{\cos^2\varphi} +\\
+\frac{r}{\cos^2\varphi}\left(P - \mu h\ddot{W}\right) = 0.
\end{aligned} \tag{9}$$

This equation will be called the equation of motion.

IV. The Yield Condition and the Associated Flow Law

The physical behavior of a solid or a structure can be prescribed with the aid of the yield condition and the yield surface. It is known that the yield surface is a closed convex surface in the space of generalized stresses. Since the exact yield surface in the space of generalized stresses is of complicate structure even in the case when the original condition in the space of principal stresses is piece wise linear many attempts have been made in order to get simple approximations of the yield surface (see Kaliszky [6], Chakrabarty [1], Skrzypek and Hetnarski [19], Jones [5]). In order to get the maximal simplicity Hodge [3] suggested the

idea of the approximation of the yield surface with "limited interaction between membrane forces and bending moments".

In the latter case two yield loci are presented independently on the planes of bending moments and membrane forces, respectively.

Following Hodge [3] and Jones [5] we assume that the yield loci are presented by quadrangles on planes N_1, N_2 and M_1, M_2 respectively. On the planes of non-dimensional stress resultants one has squares $ABCD$ (Fig. 3) and $A_1B_1C_1D_1$ (Fig. 4).

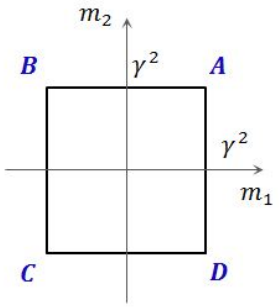

Fig. 3. Generalized square yield condition

Here the following notation is introduced

$$n_{1,2} = \frac{N_{1,2}}{N_*}, \quad m_{1,2} = \frac{M_{1,2}}{M_*}, \qquad \gamma = \frac{h}{h_*}. \tag{10}$$

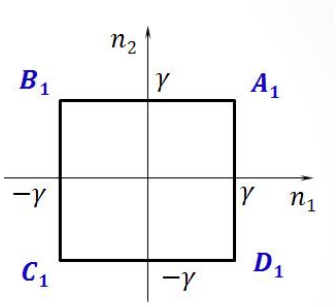

Fig. 4. Generalized square and diamond yield condition

In (10) M_* and N_* are the limit moment and limit force, respectively. It is well known that (Jones [5], Kaliszky [6])

$$M_* = \frac{\sigma_0}{4}h_*^2, N_* = \sigma_0 h_*,$$

σ_0 being the yield stress of the material.

One has to take into account that the thickness of the shell wall is piece wise constant and h_* is one of the thicknesses $h_0, \dots, h_n$. It is reasonable to choose

$$h_* = \max_{0 \le i \le n} h_i$$

and to use the notation

$$M_{0j} = \frac{\sigma_0}{4}h_j^2, \ \ N_{0j} = \sigma_0 h_j. \tag{11}$$

It is well known in the theory of plasticity that the stress state of a body corresponds to a point lying inside the yield surface or on the yield surface. In the latter case the associated flow law states that the vector of strain rates is directed towards the external normal at each regular point of the yield surface (Jones [5], Chakrabarty [1]). At the non-regular points of the yield surface the strain rate vector is defined as a linear combination of these vectors calculated for adjacent pieces of the yield surface at this point.

The deepened analysis shows that the stress profile could lie on sides AB (Fig. 3) and A_1B_1(Fig. 4) of the yield loci. For these regimes it immediately follows from the associated flow law that

$$\dot{\varkappa}_1 = 0 \tag{12}$$

and $\dot{\varkappa}_2 \ge 0$ according to Fig. 3 whereas $\dot{\varepsilon}_2 \ge 0$ and $\dot{\varepsilon}_1 = 0$ in the case of the generalized square yield condition.

Making use of (7) and (12) one obtains after double integration with respect to r

$$\dot{W} = f_1(t)r + f_2(t) \tag{13}$$

where f_1 and f_2 are arbitrary functions of time t. Introducing the notation

$$\dot{W}(a,t) = \dot{W}_0(t) \tag{14}$$

and taking into account the boundary requirement at the simply supported edge

$$\dot{W}(R,t) = 0 \tag{15}$$

one can easily deduce from (13)-(15) that

$$\dot{W}(r,t) = \dot{W}_0(t)\frac{r-R}{a-R}. \tag{16}$$

The equation $\dot{\varepsilon}_1 = 0$ with (7) and the boundary condition

$$\dot{U}(R,t) = 0 \tag{17}$$

yields the trivial solution $\dot{U} = 0$.

Note that in the case when (17) is not valid (in another support conditions) the displacement rate $\dot{U}$ may remain unspecified.

V. Integration of The Equations of Motion

It was assumed above that the stress-strain state of the shell corresponds to the horizontal sides AB and $A_1B_1$of the yield squares on planes of moments and membrane forces, respectively (Fig. 3, 4). Thus in each region $r \in (a_j, a_{j+1})$ where $j = 0, \dots, n$ one has $M_2 = M_{0j}$ and $N_2 = N_{0j}$.

Thus

$$N_2 = N_{0j}, M_2 = M_{0j} \tag{18}$$

for $r \in (a_j, a_{j+1})$; $j = 0, \dots, n$. Inserting (18) in the first equation in (8) one easily obtains after integration

$$N_1 = N_{0j} + \frac{C_j}{r} \tag{19}$$

for $r \in (\alpha_j, \alpha_{j+1})$. In (19) C_j stand for arbitrary constants. Evidently, at the internal edge $N_1(a)$ must vanish. Thus $C_0 = -N_{00}a_0$ and

$$N_1 = N_{00} - N_{00}\frac{a_0}{r} \tag{20}$$

for $r \in (a_0, a_1)$. Making use of the continuity of the membrane force N_1 at $r = a_{j+1}$ one can write

$$C_{j+1} = C_j + a_{j+1}(N_{0j} - N_{0j+1}) \tag{21}$$

for each $j = 0, \dots, n$. Making use of the recurrent relations (21) one obtains

$$C_j = -N_{00}a_0 + \sum_{i=1}^{j} a_i(N_{0i-1} - N_{0i}). \tag{22}$$

Substituting (22) into (19) results in

$$N_1 = N_{0j} + \frac{1}{r}\left[-N_{00}a_0 + \sum_{i=1}^{j} a(N_{0i-1} - N_{0i})\right] \tag{23}$$

for $r \in (a_j, a_{j+1})$; $j = 0, \dots, n$.

It follows from (16) that the acceleration can be presented as

$$\ddot{W} = \ddot{W}_0\frac{r-R}{a-R} \tag{24}$$

for $r \in (a, R)$.

Substituting (18) and (24) in (9) after integration with respect to r one obtains

$$[(rM_1)' - M_2]\cos^2\varphi - N_{0j}r\sin\varphi + \\ + P\frac{r^2}{2} - -\frac{\mu h_j\ddot{W}_0}{a-R}\left(\frac{r^3}{3} - \frac{Rr^2}{2}\right) + B_j = 0, \tag{25}$$

for $r \in (a_j, a_{j+1})$; $j = 0, \dots, n$. Here B_j stand for arbitrary constants.

Because of the continuity of the shear force, or the quantity in square brackets at $r = a_{j+1}$ one can write

$$B_{j+1} = B_j + (N_{0j+1} - N_{0j})a_{j+1}\sin\varphi + \\ + \frac{\mu\ddot{W}_0}{a-R}\left(\frac{a_{j+1}^3}{3} - \frac{Ra_{j+1}^2}{2}\right)(h_{j+1} - h_j) \tag{26}$$

for each $j = 0, \dots, n-1$. Thus, it infers from (26) that

$$B_j = B_0 + \sum_{i=1}^{j}\left[(N_{0i} - N_{0i-1})a_i\sin\varphi \right. \\ \left. + \frac{\mu\ddot{W}_0}{a-R}\left(\frac{a_i^3}{3} - \frac{Ra_i^2}{2}\right)(h_i - h_{i-1})\right], \tag{27}$$

where

$$B_0 = N_{00}a\sin\varphi - \frac{P}{2}a^2 + \frac{\mu\ddot{W}_0h_0}{a-R}\left(\frac{a^3}{3} - \frac{Ra^2}{2}\right). \tag{28}$$

The integration of (25) immediately gives

$$[rM_1 - M_{0j}r]\cos^2\varphi - N_{0j}\frac{r^2}{2}\sin\varphi + P\frac{r^3}{6} - \\ - \frac{\mu h_j\ddot{W}_0}{a-R}\left(\frac{r^4}{12} - \frac{Rr^3}{6}\right) + B_jr + A_j = 0, \tag{29}$$

for $r \in (a_j, a_{j+1})$; $j = 0, \dots, n$. Since the bending moment M_1 is continuous everywhere, it must be continuous at $r = a_{j+1}$. Due to the continuity of M_1 at $r = a_{j+1}$ one has

$$-M_{0j+1}a_{j+1}\cos^2\varphi - \frac{1}{2}N_{0j+1}a_{j+1}^2\sin\varphi + B_{j+1}a_{j+1} + \\ + A_{j+1} - -\frac{\mu\ddot{W}_0}{a-R}\left(\frac{a_{j+1}^4}{12} - \frac{Ra_{j+1}^3}{6}\right)h_{j+1} = \\ = -M_{0j}a_{j+1}\cos^2\varphi - \frac{1}{2}N_{0j}a_{j+1}^2\sin\varphi + B_ja_{j+1} + \\ + A_j - \frac{\mu\ddot{W}_0}{a-R}\left(\frac{a_{j+1}^4}{12} - \frac{Ra_{j+1}^3}{6}\right)h_j \tag{30}$$

Thus

$$A_{j+1} = A_j + a_{j+1}(M_{0j+1} - M_{0j})\cos^2\varphi + \\ + \frac{1}{2}a_{j+1}^2(N_{0j+1} - N_{0j})\sin\varphi + a_{j+1}(B_j - B_{j+1}) \\ + \frac{\mu\ddot{W}_0}{a-R}\left(\frac{a_{j+1}^4}{12} - \frac{Ra_{j+1}^3}{6}\right)(h_{j+1} - h_j) \tag{31}$$

for $j = 0, \dots, n-1$.

At the free edge the radial bending moment must vanish. Taking this into account one obtains from (28), (29)

$$A_0 = -\frac{a^2}{2}N_{00}\sin\varphi + \frac{P}{3}a^3 + \\ + \frac{\mu\ddot{W}_0h_0}{a-R}\left(-\frac{a^4}{4} + \frac{Ra^3}{3}\right) + aM_{00}\cos^2\varphi \tag{32}$$

Combining (27), (31), (32) one obtains

$$A_j = A_0 + \sum_{i=1}^{j}\left[a_i(M_{0i} - M_{0i-1})\cos^2\varphi - \right. \\ - \frac{a_i^2}{2}(N_{0i} - N_{0i-1})\sin\varphi \\ \left. - \frac{\mu\ddot{W}_0}{a-R}\left(\frac{a_i^4}{4} - \frac{Ra_i^3}{3}\right)(h_i - h_{i-1})\right] \tag{33}$$

for $j = 1, \dots, n$.

Substituting (27), (28) and (31)-(33) in (29) one can define the bending moment

$$M_1 = M_{0j} + \frac{1}{\cos^2\varphi}\left\{\frac{r}{2}N_{0j}\sin\varphi - P\frac{r^2}{6} + \frac{\mu h_j \ddot{W}_0}{a-R}\left(\frac{r^3}{12} - \frac{Rr^2}{6}\right)\right\} - \tag{34}$$
$$-\frac{1}{\cos^2\varphi}\left\{\sum_{i=1}^{n}\frac{\mu\ddot{W}_0}{a-R}\left(\frac{a_i^3}{3} - \frac{Ra_i^2}{2}\right)(h_i - h_{i-1}) - B_0 - \sum_{i=1}^{j} a_i(N_{0i} - N_{0i-1})\sin\varphi - \frac{1}{r}A_0\right\} -$$
$$-\frac{1}{r\cos^2\varphi}\sum_{i=1}^{j}\left[a_i(M_{0i} - M_{0i-1})\cos^2\varphi - \frac{a_i^2}{2}(N_{0i} - N_{0i-1})\sin\varphi - \frac{\mu\ddot{W}_0}{a-R}\left(\frac{a_i^4}{4} - \frac{Ra_i^3}{3}\right)(h_i - h_{i-1})\right]$$

for $r \in [a_j, a_{j+1}]$; $j = 0, \dots, n$. Note that in (34) and elsewhere the following rule of summation is assumed to hold good, namely

$$\sum_{i=1}^{0} z_i = 0,$$

where z_i is an arbitrary member of the summation.

It follows from (34) that the boundary condition $M_1(R,t) = 0$ is satisfied if

$$RM_{n0} + \frac{N_{n0}R^2}{2} - \frac{PR^3}{6} - \frac{\mu\ddot{W}_0 h_n R^3}{12(a-R)} - \sum_{i=1}^{n}\left[\frac{\mu\ddot{W}_0 R}{a-R}\left(\frac{a_i^3}{3} - \frac{Ra_i^2}{2}\right)(h_i - h_{i-1})\right] - \tag{35}$$
$$-RB_0 - A_0 - \sum_{i=1}^{n}\left[\left(Ra_i - \frac{a_i^2}{2}\right)(N_{0i} - N_{0i-1})\sin\varphi + a_i(M_{0i} - M_{0i-1})\cos^2\varphi - \frac{\mu\ddot{W}_0}{a-R}\left(\frac{a_i^4}{4} - \frac{Ra_i^3}{3}\right)(h_i - h_{i-1})\right] = 0.$$

Substituting the constants A_0 and B_0 from (28) and (32) in (35) one can define the acceleration

$$\mu\ddot{W}_0 = \frac{a-R}{12T}\left\{-RM_{n0} - \frac{R^2}{2}N_{n0} + \frac{PR^3}{6} - \frac{a^2}{2}N_{00} - \frac{Pa^3}{3} - \sum_{i=1}^{n}(N_{0i} - N_{0i-1})\left(Ra_i - \frac{a_i^2}{2}\right)\sin\varphi + a_i(M_{0i} - M_{0i-1})\right\} \tag{36}$$

where for the conciseness sake the following notation is used

$$T = -Rh_0\left(\frac{a^3}{3} - \frac{Ra^2}{2}\right) + \frac{a^4}{4} - \frac{Ra^3}{3} + \sum_{i=1}^{n}(h_i - h_{i-1})\left(\frac{a_i^4}{4} - \frac{R^2a_i^2}{2}\right). \tag{37}$$

VI. Determination of Residual Deflections

According to the assumptions made above the deflection rates at each point of the shell are defined by (16) where $\dot{W}_0$ is the transverse velocity at the free edge of the shell as shown by (14).

One can easily recheck that for each $t \geq t_*$ this quantity can be determined with the help of the acceleration as

$$\dot{W}_0(t,P) = \int_{t_*}^{t}\ddot{W}_0(\tau,P)d\tau + \dot{W}_0\big(t_*, P(t_*)\big) \tag{38}$$

where $t_* > 0$ is an arbitrary instant of time. Let us study the both stages of deformation in the greater detail.

A. The first stage ($0 \leq t \leq t_0$)

During this stage the shell is subjected to the blast loading of intensity $P = p_0 g(t)$. Taking $t_* = 0$ in (38) and bearing in mind that

$$\dot{W}_0(0) = 0, W_0(0) = 0 \tag{39}$$

one immediately obtains

$$\dot{W}_0(t) = \int_0^t \psi(\tau,P)d\tau \tag{40}$$

and

$$W_0(t) = \int_0^t\int_0^\tau \psi(\xi,P)d\xi d\tau \tag{41}$$

where

$$\psi\big(t,P(t)\big) = \ddot{W}_0(t). \tag{42}$$

The function $\psi\big(t,P(t)\big)$ can be determined from (36) making use of (2) and (37).

From (40)-(42) one can easily find

$$\dot{W}_0(t_0) = \int_0^{t_0}\psi(\tau,P)\,d\tau \tag{43}$$

and

$$W_0(t_0) = \int_0^{t_0}\int_0^\tau \psi(\xi,P)d\xi d\tau. \tag{44}$$

The values of the deflection and its velocity given by (43), (44) will be used as initial conditions for the second stage of deformation.

B. The second stage $(t_0 \le t \le t_1)$

It is assumed that at the moment $t = t_0$ the transverse loading is abrupt-wisely removed and the subsequent motion takes place due to the inertia. During the final stage of motion $P = 0$ and thus according to (38) $t = t_*$ and the velocity is to be calculated as (here $t \in [t_0, t_1]$)

$$\dot{W}_0(t) = \int_{t_0}^{t} \psi(\tau, 0)d\tau + \dot{W}_0(t_0). \quad (45)$$

Similarly, the transverse deflection during this stage is

$$W_0(t) = \int_{t_0}^{t}\int_{t_0}^{\tau} \psi(\xi, 0)d\xi d\tau + \dot{W}_0(t_0)(t - t_0) + W_0(t_0). \quad (46)$$

The motion ceases at the moment $t = t_1$ when $\dot{W}_0(t_1) = 0$. The quantity t_1 is calculated from the equation

$$\int_{0}^{t_0} \psi\left(\tau, P(\tau)\right)d\tau + \int_{t_0}^{t_1} \psi(\tau, 0)d\tau = 0. \quad (47)$$

Making use of (40), (41), (45) one can determine the maximal residual deflection as

$$W_0(t_1) = \int_{t_0}^{t_1}\int_{t_0}^{\tau} \psi(\xi, 0)d\xi d\tau + \int_{0}^{t_0} \psi\left(\tau, P(\tau)\right)d\tau(t_1 - t_0) + W_0(t_0), \quad (48)$$

where the last term is to be calculated from (46) for $t = t_0$.

Making use of (16) and (48) one can calculate residual deflections at each $r \in [a, R]$ as

$$W(r, t_1) = W_0(t_1)\frac{r - R}{a - R}. \quad (49)$$

The residual deflections have been calculated in a greater detail in the case when

$$P(t) = p_0 e^{-\beta t}$$

during the loading stage of deformation.

VII. Numerical Results and Discussion

The deflections of the shell at the free edge and at $r = a_1$ are shown in Fig. 5. Here the dashed lines correspond to the shell with constant thickness h_0, whereas solid lines are associated with stepped shells $(h_1/h_0 = 2)$. As it might be expected the higher couple of curves presents the transverse deflections at the free edge of the shell whereas the lower pair of curves corresponds to the circle where the step is located. It can be seen from Fig. 5 that in both cross sections of the shell the transverse displacements monotonically increase during the first stage of deformation.

The variation of the radial bending moment with the variation of the load intensity is shown in Fig. 6. Fig. 6 is calculated for a shell with piece wise constant thickness with two thicknesses and the step at $a_1 = 0{,}55R$. Here $h_1 = 1{,}5h_0; k = 0{,}3$ whereas

$$p = \frac{PR}{M_{00}\sin\varphi}; k = \frac{M_{00}\cos\varphi}{RN_{00}\sin\varphi}.$$

In Fig. 6-11 the following notation is used

$$m_1 = \frac{M_1}{M_{00}}, \varrho = \frac{r}{R}, \alpha = \frac{a}{R}, W_2 = W(a, t_1)$$

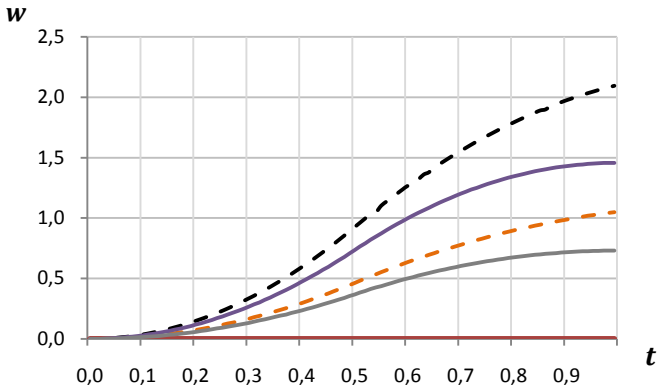

Fig. 5. Deflections at $r = a$ and $r = a_1$

It can be seen from Fig. 6 that the higher is the pressure loading the higher is the radial bending moment, as might be expected. The curves depicted in Fig. 6 have slope discontinuities at $r = 0{,}55R$.

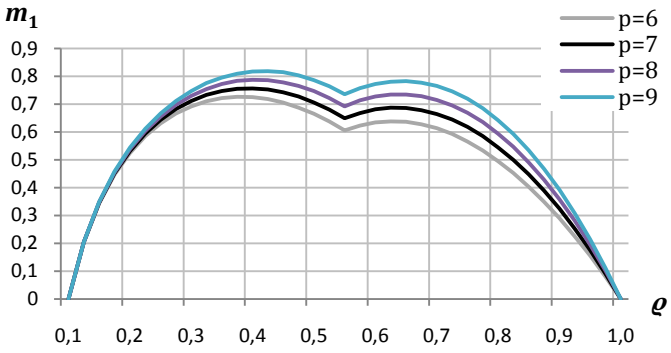

Fig. 6. Bending moment distributions

The discontinuities are caused by the step of the thickness.

The radial bending moment distributions are shown for blast loaded shells at $t = t_0$ and $t = t_1$ in Fig. 7 and Fig. 8, respectively. Solid lines in Fig. 7, 8 correspond to shells with two steps located at $r = 0{,}6R$ and $r = 0{,}65R$, respectively. The dashed lines correspond to the shell of constant thickness. The considered shells have the ratios of thicknesses $h_1 = 2h_0, h_1 = 1{,}5h_0$ and $h_1 = 1{,}25h_0$, respectively.

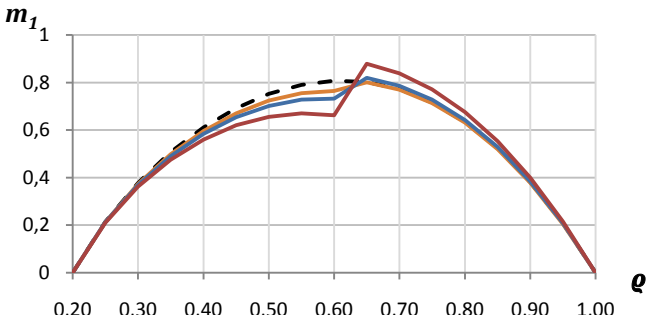

Fig. 7. Bending moment distributions at $t = t_0$

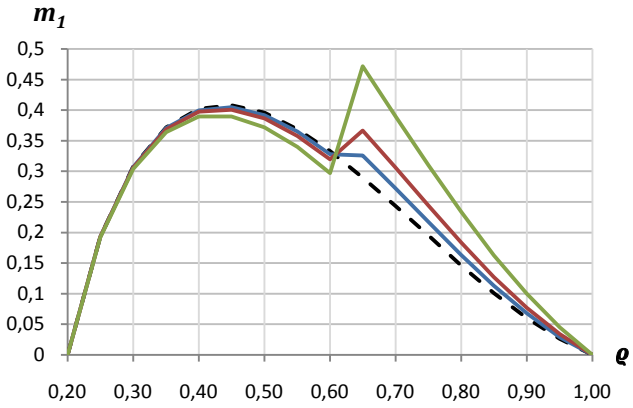

Fig. 8. Bending moment distributions at $t = t_1$

The maximal residual deflections for different inner radii and different loading times are shown in Fig. 9 and Fig. 10. In Fig. 10 dashed lines correspond to shells with two steps (here $\alpha_1 = 0{,}6$; $\alpha_2 = 0{,}65$) and the solid lines correspond to shells with a unique step. Here the corresponding couples of curves are associated with the loading time $t_0 = 0{,}3; t_0 = 0{,}4$ and $t_0 = 0{,}5$, respectively. In the case of solid lines $h_1 = 1{,}2h_0$. However, in the case of dashed lines $h_1 = 2h_0$. It can be seen from Fig. 9 that the longer is the loading period the greater is the residual deflection of the shell, as might be expected.

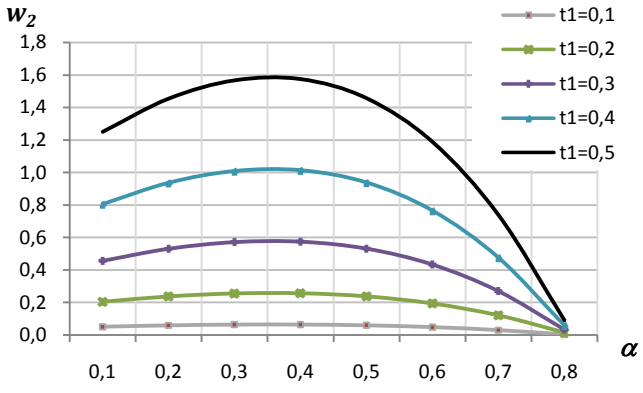

Fig. 9. Maximal residual deflections for different inner radii

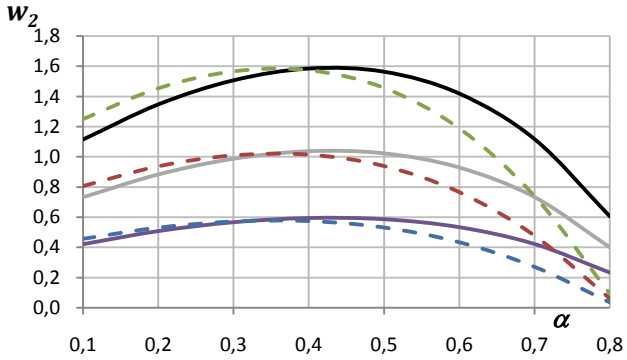

Fig. 10. Maximal residual deflections for different thicknesses

It is interesting to mention that the static limit load for a conical shell subjected to the uniformly distributed lateral loading can be obtained from (36) taking $\dot{W} = 0$. The limit loads of the open shell calculated by the current method are compared with the results of Xu et al [23] in Fig. 11. Calculations carried out showed that the results are quite close to each other.

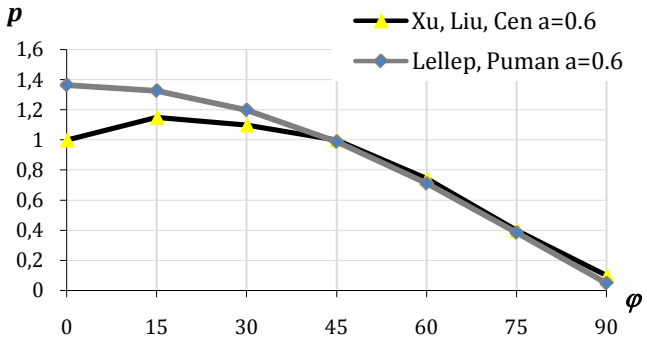

Fig. 11. Limit loads

VIII. Conclusions

Making use of an approximation of the exact yield surface an approximate method for determination of residual deflections of conical shells was developed. The shells under consideration are subjected to the blast loading. Statically admissible distributions of generalized stresses have been found under the assumption that the material of the shell is a perfect plastic material. The obtained solution is an exact solution in the range of moderate values of the load intensities. In the case of very high pressure loadings this approach leads to approximate values of residual deflections. In the future this method will be used for determination of residual deflections of shells with continuously variable thicknesses. In this case one has to approximate the variable thickness to a piece wise constant one with appropriate thicknesses and step coordinates.

REFERENCES

[1] J. Chakrabarty, *Theory of Plasticity*, Elsevier, 2006.

[2] T.A. Duffey, Dynamic rupture of shells, *Structural Failure* (Ed-s T.Wierzbicki, N.Jones), Wiley, 1999, pp. 161–192.

[3] P.G. Hodge, *Limit Analysis of Rotationally Symmetric Shells*, New Jersey: Prentice Hall, 1963.

[4] H.G. Hopkins and W. Prager, On the dynamics of plastic circular plates. *ZAMP*, 1954, 5, pp. 317–330.

[5] N. Jones, *Structural Impact*, CUP: Cambridge, 2011.

[6] S. Kaliszky, *Plasticity. Theory and Engineering Applications*, Amsterdam: Elsevier, 1989.

[7] R.W. Kuech and S.L. Lee, Limit analysis of simply supported conical shells subjected to uniform internal pressure, *Journal of the Franklin Institute*, 1965, 280, 1, pp. 71–87.

[8] R.H. Lance and C.H. Lee, The yield point load of a conical shell, *International Journal of Mechanical Sciences*, 1969, 11, 1, pp. 129–143.

[9] J. Lellep and E. Puman, Optimization of plastic conical shells of piece wise constant thickness. *Structural Optimization*, 1999, 18, pp. 74–79.

[10] J. Lellep and E. Puman, Optimization of inelastic conical shells with cracks. *Structural and Multidisciplinary Optimization*, 2007, 33, pp. 189–197.

[11] J. Lellep and E. Puman, Optimization of elastic and inelastic conical shells of piece wise constant thickness. *Recent Researches in Mechanics: 2nd International Conference on Theoretical and Applied Mechanics*, WSEAS, 2011, pp. 223–228.

[12] J. Lellep and E. Puman, Optimization of conical shells of piece wise constant thickness. WSEAS Transactions on Mathematics, WSEAS, 2012,11(3), pp. 242–251.

[13] J. Lellep and E. Puman, Plastic behaviour of stepped conical shells under impact loading, *WIT Transactions on the Built Environment*, 2012, 126, pp. 15–25.

[14] J. Lellep and E. Puman, Blast loading of inelastic conical shells with stiffeners. *Recent Advances in Mechanical Engineering*, WSEAS, 2014, pp. 77–83.

[15] J.B. Martin, *Plasticity: Fundamentals and General Results*, MIT Press, 1975.

[16] E.T. Onat, Plastic analysis of shallow conical shells, *Proceedings of ASCE*, 1960, EM6, pp. 1–12.

[17] C.T.F. Ross, *Pressure Vessels under External Pressure: Statics and Dynamics*, Elsevier: London, 1990.

[18] W.Q. Shen and N. Jones, Dynamic response and failure of fully clamped circular plates under impulse loading. *International Journal of Impact Engineering*, 1993, 13, pp. 259–278.

[19] J.J. Skrszypek and R.B. Hetnarski, *Plasticity and Creep. Theory, Examples and Problems*, CRC Press, Boca Raton, 1993.

[20] W. Stronge and T.X. Yu, *Models of Dynamic Plasticity*, Springer Verlag, 1993.

[21] J. R. Vinson, *Plate and Panel Structures of Isotropic, Composite and Piezoelectric Materials, Including Sandwich Construction*, Springer, Dordrecht, 2005.

[22] H.M. Wen, T.X. Yu and T.Y. Reddy, A note on clamped circular plates under impulsive loading. *Mechanics of Structures and Machines*, 1995, 23, 331–342.

[23] B. Xu, , Y. Liu, and Z. Cen, Some developments in limit analysis solutions of structures. *Metals and Materials*, **4**(3), 1998, pp. 329–335.